Ann. Occup. Hyg., Vol. 55, No. 7, pp. 784–796, 2011
Published by Oxford University Press
on behalf of the British Occupational Hygiene Society
doi:10.1093/annhyg/mer062

A Recirculation Aerosol Wind Tunnel for Evaluating Aerosol Samplers and Measuring Particle Penetration through Protective Clothing Materials

PETER A. JAQUES[1], TA-CHIH HSIAO[2,3] and PENGFEI GAO[2]*

[1]URS Corporation, 626 Cochrans Mill Road, Pittsburgh, PA 15236, USA; [2]National Institute for Occupational Safety and Health, National Personal Protective Technology Laboratory, 626 Cochrans Mill Road, Pittsburgh, PA 15236, USA

Received 16 March 2011; in final form 11 April 2011

A recirculation aerosol wind tunnel was designed to maintain a uniform airflow and stable aerosol size distribution for evaluating aerosol sampler performance and determining particle penetration through protective clothing materials. The oval-shaped wind tunnel was designed to be small enough to fit onto a lab bench, have optimized dimensions for uniformity in wind speed and particle size distributions, sufficient mixing for even distribution of particles, and minimum particle losses. Performance evaluation demonstrates a relatively high level of spatial uniformity, with a coefficient of variation of 1.5–6.2% for wind velocities between 0.4 and 2.8 m s^{-1} and, in this range, 0.8–8.5% for particles between 50 and 450 nm. Aerosol concentration stabilized within the first 5–20 min with, approximately, a count median diameter of 135 nm and geometric standard deviation of 2.20. Negligible agglomerate growth and particle loss are suggested. The recirculation design appears to result in unique features as needed for our research.

Keywords: aerosols; aerosol chamber; aerosol samplers; protective clothing; particle penetration; wind tunnel

INTRODUCTION

Currently, research is underway to develop innovative test methods for personal protective equipment. A recirculation aerosol wind tunnel (RAWT) was designed and characterized to optimize uniform flow and consistent aerosol conditions for the evaluation of a magnetic passive aerosol sampler (MPAS) and for measuring nano- and submicron particle penetration through protective clothing materials (Gao *et al.*, 2011). The U.S. Environmental Protection Agency (EPA) (1987, 1997) specifies that wind tunnels and aerosol monitors tested within them have a spatial variability no greater than 10%. Within the central two-thirds of a 1.83 m diameter, 11 m long, circular closed loop wind tunnel for wind speeds between 0.56 and 6.6 m s^{-1} and for 10 μm particles within this range, Cheng *et al.* (2004) found the coefficient of variation (CV) to be <5% for wind speed and 7.5 and 9.1% for particles. Similarly, Ranade *et al.* (1990) and Hinds and Kuo (1995) reported aerosol testing wind tunnels of different dimensions to have <10% CV for both parameters. To meet cost and space limitations, Eddins *et al.* (1996) designed a compact wind tunnel with an arrangement of three jet pumps for evaluating aerosol samplers. To characterize a non-magnetic passive aerosol sampler, Peters and Leith (2004a,b,c) designed an aerosol supply and delivery system using gored (welded) and smooth pipes with a curvature ratio (radius-of-bend to duct-radius) of ∼3. The design of our wind tunnel took into consideration several of the parameters used by the aforementioned studies.

Conventional passive aerosol samplers have low collection efficiency, requiring days or weeks to sample an adequate concentration of particles for

*Author to whom correspondence should be addressed; Tel: 412-386-6885; fax: 412-386-4089; e-mail: PGao@cdc.gov
[3]Present address: National Central University, Taiwan, Republic of China.

analysis (e.g. Wagner and Leith, 2001). On the other hand, most protective clothing materials have relatively high-capture efficiency and particle penetration is primarily driven by wind (Bergman *et al.*, 1989; U.S. Army Dugway Proving Ground UT, 1997; IEST, 2003; Gao *et al.*, 2011). The MPAS, to be described in another paper, was developed to monitor particle penetration through protective ensembles worn by human subjects or through clothing materials in a chamber. To enhance its collection efficiency, it uses a magnetic backing plate to collect magnetically susceptible aerosol particles. The MPAS is a 28 mm diameter and 8.6-mm thick disc, which uses ~140 square magnets (1.5 × 1.5 × 0.71 mm), arranged in alternating adjacent N and S poles, to form a 20 mm diameter (314 mm^2) multidomain collection surface. Prior to application testing, the collection response of the MPAS needed to be characterized. To test its performance and measure particle penetration through clothing materials, the RAWT was designed as a close-looped system to overcome inherent particle losses and maintain a sufficient aerosol concentration. Because moderate-to-high wind velocities can be encountered in the workplace, the RAWT was evaluated at a range of wind conditions. The objectives in the development of the RAWT were to provide a moderately high aerosol, stable in concentration and size distribution, with good uniformity of concentration and velocity across the test section within the available lab space.

MATERIALS AND EXPERIMENTAL METHODS

RAWT design

The RAWT (Vandiver Enterprises, Zelienople, PA, USA) is a benchtop low-velocity closed loop (recirculation) wind tunnel (Gao *et al.*, 2011). The detailed dimensions and setup of the unit are shown in a schematic diagram and photograph (Figs 1a and b). The tunnel flow is controlled by a variable speed fan-driven power ventilator (Model FKD 10; Fantech, Sarasota, FL, USA). The air blower, located in the upper section, forces aerosol through the experimental test section, located in the lower section, for its first pass, which recombines it with freshly injected aerosol at each subsequent pass, serving to concentrate the aerosol. The tunnel consists of two parallel ducts, connected by gored turns with a curvature ratio of 1 (0.25:0.25 m). The overall dimensions of the system are 4.6 m long by 0.84 m high. The top section and elbows are each 0.25 m in diameter and the bottom section is 0.38 m in diameter.

While gradual (20% grade) transition zones were designed to minimize turbulence and particle losses, inherent turbulent mixing of the aerosol was expected to effectively create a spatially uniform particle size distribution (PSD). The test sections are offset from the center to maximize travel distance from the unit's elbow and therefore increase the length-to-diameter ratio to reach fully developed flow. The features of smooth surfaces, subtle changes in dimensions and a circular cross section were intended to reduce turbulence and particle losses. A honeycomb flow straightener was placed ~2 m upstream of the test section and two medium meshed screens placed immediately up- and downstream of the test section to enhance flow straightening and allow for uniform particle measurements by the MPAS, regardless of its orientation.

Aerosol generation and injection apparatus

Details of the aerosol generation system are provided in an earlier paper (Gao *et al.*, 2011). Polydisperse iron (II, III) oxide (i.e. Fe_3O_4, 5.2 g cm^{-3}) particles were generated using a six-jet atomizer (Model 9306; TSI Incorporated, Shoreview, MN, USA) (see Fig. 1c). Iron (II, III) oxide particles are magnetically susceptible, which does not affect intra-particle attractions and, thus, neither agglomeration losses nor growth. This susceptibility enhances the particle's force of attraction for magnetic surfaces and is, thus, optimal for particle collection onto the MPAS. A benchtop rotational shaker (Innova 2300; New Brunswick Scientific, Edison, NJ, USA) was used to maintain particle suspension during the generation process. Two diffusion dryers, each with water traps (Model 3062; TSI Incorporated) were used to remove moisture, and a neutralizer (Model 3012; TSI Incorporated) were used to minimize electrostatic effects. The particles were injected into the RAWT 1 m upstream of the fan, and excess air was exhausted to maintain static pressure within the tunnel.

Performance evaluation criteria

The U.S. EPA equivalent method specifies a test procedure for determining the stability of aerosol sampling and airflow in the measurement of particulate matter <10 μm in aerodynamic diameter (PM_{10}) (U.S. EPA, 1987; Ranade, 1990). A similar test procedure and method for the full wind tunnel test is specified separately (U.S. EPA, 1997). The EPA documents specify that the air velocity and aerosol throughout the test section of the wind tunnel should be within 10% of their mean. An array of at least five evenly spaced isokinetic samplers should be used to determine the particle concentration profile in the sampling zone of the wind tunnel, and the

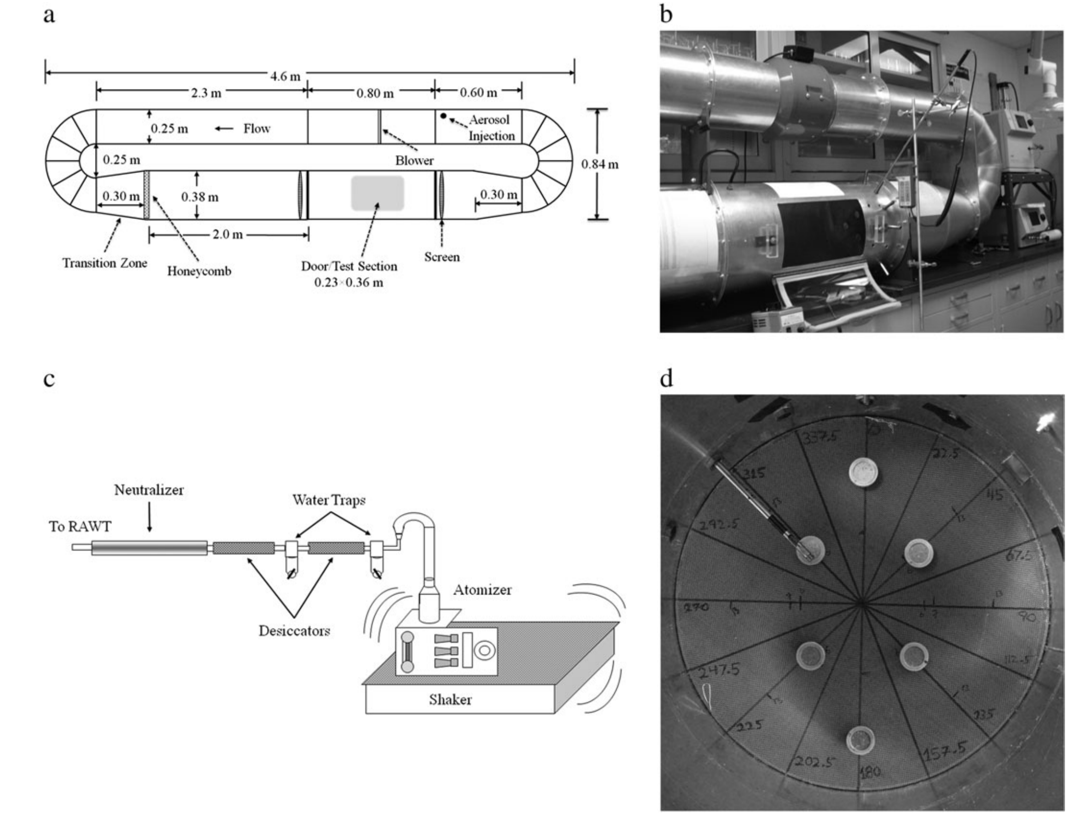

Fig. 1. (a) Schematic of the RAWT, (b) photograph of aerosol test section and blower, (c) aerosol generation and delivery system, and (d) velocity measurement probe with six MPASs placed on screened test section.

measurements should be performed at velocities of 0.6, 2.2 and 6.6 m s^{-1}.

Although the RAWT was designed for the characterization of the MPAS and testing of clothing materials rather than for testing of an active ambient PM_{10} sampler, the EPA's performance criteria serves as a useful guide rather than a strict regulation, especially since there are no current reference methods for testing the effectiveness of passive aerosol samplers and clothing materials on collecting submicrometer and nanoparticles in a wind tunnel. Thus, much of the EPA's testing criteria was considered in the design and evaluation of the RAWT, including positioning of the velocity probes and particle samplers (albeit, in a radial, rather than rectangular grid), and the applied wind speeds (0.4–3.2 m s^{-1}), which span half the lower end of the range specified by the EPA. As in similar studies, average wind velocities and particle concentrations were measured. The upper wind limit used by the EPA was established for ambient high volume particulate samplers, while the upper wind speed in this study was used to simulate typical wind conditions experienced by workers. As in similar studies, the uniformity of the data is reported as %CV (e.g. Ranade *et al.*, 1990; Eddins *et al.*, 1996; Cheng *et al.*, 2004).

Determination of spatial uniformity of air velocity

The air velocity profile was tested using a velometer (Model 8386A, VelociCalc Plus; TSI Incorporated) on a circular cross section immediately upstream of the second flow straightening fine mesh screen. Measurements were made at five blower voltage settings (20, 40, 60, 80, and 100 V) along several radial segments, transecting at 0.04, 0.10, and 0.17 m from the center axis, which is 0.19 m from the walls of the 0.38-m diameter tunnel (see Fig. 1d). The segments span 360° around the tunnel and are separated by either 22.5- or 45° intervals (22.5, 45, 90, 135, 157.5, 202.5, 225, 270, 315, and 337.5°), which are additionally illustrated in a radial data graph presented in the Results section. For data analysis purposes, a set of measurements at a given coordinate are defined by the segment angle and its distance from the origin. For example, 270_10 represents measurements at 10 cm from the center along the 270°

segment, which is horizontal (level to the bench) and ends at the back wall of the tunnel. The objective was to measure a full range of coordinates of a circular cross section that could define the spatial uniformity of airflow and allow for several collocated MPAS sampler test points. The relationship between blower setting and wind speed was measured and used as a reference for setting desired experimental wind speeds. Wind speed increased linearly with power at all coordinates measured. For power settings between 20 and 100 V, the center-origin wind velocity ranged from 0.4 to 3.2 m s^{-1} and varied linearly according to center-origin wind velocity (m s^{-1}) = 0.035 × voltage (V) – 0.339, with a R^2 = 0.997.

Turbulence in the tunnel can contribute to non laminar flow, which, desirably, causes mixing and enhances spatial uniformity of particle concentration. However, since face velocity affects sampling efficiency of a blunt body, such as the MPAS (Dandy and Yu, 1997), spatially nonuniform airflow may cause variability between collocated MPASs within the test section (Lidén and Kenny, 1994; Aizenberg *et al.*, 2001). Regardless of the expected turbulence, the distribution of flow within the tolerance limits specified by the U.S. EPA (1987, 1997) was considered adequate for producing comparable particle collection results with collocated MPASs. For the lowest wind setting used in this study, the Reynolds number relative to the tunnel diameter was >10 000. Thus, the full range of wind settings used was expected to result in turbulent conditions within the lower section of the RAWT. To minimize the effect of irregular flows on uniformity, as described earlier, a honeycomb and two fine mesh screens were used.

Determination of aerosol spatial uniformity

To evaluate spatial uniformity of the recirculated aerosol, a pair of identical scanning mobility particle sizers [(SMPS) Model 3936; TSI Incorporated] was used to simultaneously measure the size distribution of the polydisperse iron (II, III) oxide particles across a planar cross section in front of the second fine mesh screen of the test section at 0.8 m downstream of the test section's screened entrance (see Fig. 1). Similar to the wind measurements, one SMPS sampled at points along the radial axes and the second was used as a reference at the origin. Both were collocated for measurements made at the center of the cross section. A stainless steel sampling probe, connected to black conductive tube and the SMPS, was positioned collinearly in the horizontal upstream direction, which was assumed to be parallel with the straight walls of the tunnel and therefore parallel with the primary direction of flow. Issues for anisokinetic sampling in turbulent flow were considered. The average air speed of the SMPS sample inlet probe (with a sampling flow rate of 0.3 l.p.m.) was 0.35 m s^{-1}. Thus, for the aerosol sampling speeds delivered by the RAWT (0.4–2.8 m s^{-1}), the conditions could not be isokinetic, potentially leading to inaccurate sampling of large particles. As noted in the ANSI N13.1-1999 standard for air sampling in stacks and ducts (ANSI, 1999), a shrouded probe should be used if the aerosol to be sampled contains particles with a large enough aerodynamic diameter to have substantial inertial properties. To minimize the particle losses, the sample probe's inlet was tapered. To confirm that anisokinetic sampling was not a concern, particle Stokes number and Reynolds numbers for the upper particle size (0.5 μm) and wind speed (3.2 m s^{-1}) limits were computed as 0.006 and 0.106, respectively, showing that the effect of particle inertia on sampling efficiency can be considered negligible (Hinds, 1999). Finally, sample probe wall losses were considered. Since paired SMPSs with equivalent and minimal length tubing (56 cm) were employed, relative measurements rather than absolute concentrations were used to determine the spatial distribution of aerosol. Thus, any of the minimally expected wall losses of particles in the sample lines [~5% for 0.03 μm particles and <1% for 0.15 μm particles (Hinds, 1999)] were expected to be normalized between the two samplers and not affect the reported aerosol distribution results.

In data analysis, spatial measurements made from the second SMPS were normalized to measurements made at the center-origin by the first SMPS and reported as a unitless ratio. Spatial aerosol measurements were conducted at blower power settings of 20, 40, and 80 V along most of the same sectors as for the velocity measurements, but across different concentric circles that were slightly closer to the center axis (4, 7, and 13 cm from the center) (see Fig. 1d).

Determination of aerosol concentration stability

Since the RAWT is designed for testing aerosol collection devices and protective clothing over extended time periods, the consistency in concentrations and size distribution of delivered aerosols is critical. Coagulation causes particle size increase and number concentration decrease (Friedlander, 2000). Deposition losses of larger particles are enhanced at higher wind speeds and, conversely, losses of particles in the diffusion range are favored at very low velocities. Deposition losses were examined in this study by discontinuing injection of fresh aerosol and observing aerosol concentration decay. To evaluate coagulation effects, the PSD is evaluated over time, while fresh particles are continually injected and combined with aged aerosols.

RESULTS AND DISCUSSION

Aerosol concentration and size distribution

Figure 2 presents a typical size distribution and ratio of concentration by particle size of the aerosol at typical wind velocities of 0.32 and 2.8 m s^{-1}, which both show an average count mean diameter of 135 nm and geometric standard deviation of 2.2. The peak concentrations reached as high as 10^5 particles per cubic centimeter. A relative increase in concentration with particle size at the lower speed of ~30% at 30 nm to ~180% at 350 nm shows that there was an increase in particle loss with increasing size for the higher wind speeds, which may be due to increases in turbulent diffusion near the wind tunnel walls (Hadj and Ahmadi, 1990). The figure also shows the ratio of concentration at 0.32 m s^{-1} to that at 2.8 m s^{-1} for each particle size from 50 to 445 nm. For a single-pass wind tunnel, without considering deposition losses, an increase in wind speed from 0.32 to 2.8 m s^{-1} would be expected to cause the aerosol concentration to proportionally decrease by a factor of 7.75 due to the dilution effect of carrier air. Furthermore, with deposition, it is expected that at the higher velocities this factor would be greater. In contrast, the factors were only reduced to between 1.3 and 2.8 (as shown in Fig. 2), suggesting the recirculation design rendered a significantly higher concentration than that which could be obtained with a single-pass wind tunnel at a given aerosol generation rate.

Overall uniformity

The uniformity of the RAWT is shown in Fig. 3, which presents the CV of wind velocity as a function of blower setting along all points measured at distances from the center of the tunnel, and in Fig. 4, which shows the CV of particle number concentration as a function of particle size for all coordinates throughout the test cross section at 0.32, 1.0, and 2.8 m s^{-1}. From 0.4 to 2.8 m s^{-1}, a high level of uniformity for both number concentration (for particles with $_{em}D_{50}$ between 50 and 445 nm) and air velocity were observed.

Generally, the results show that the air velocities and particle concentrations in the experimental test section of the RAWT meet the U.S. EPA criteria for uniformity. Additionally, the uniformity of air velocity and the aerosol concentration compares well with other studies (Ranade *et al.*, 1990; Eddins *et al.*, 1996; Cheng *et al.*, 2004), although the wind tunnels used in those studies were of different dimensions [e.g. much larger in diameter (Ranade

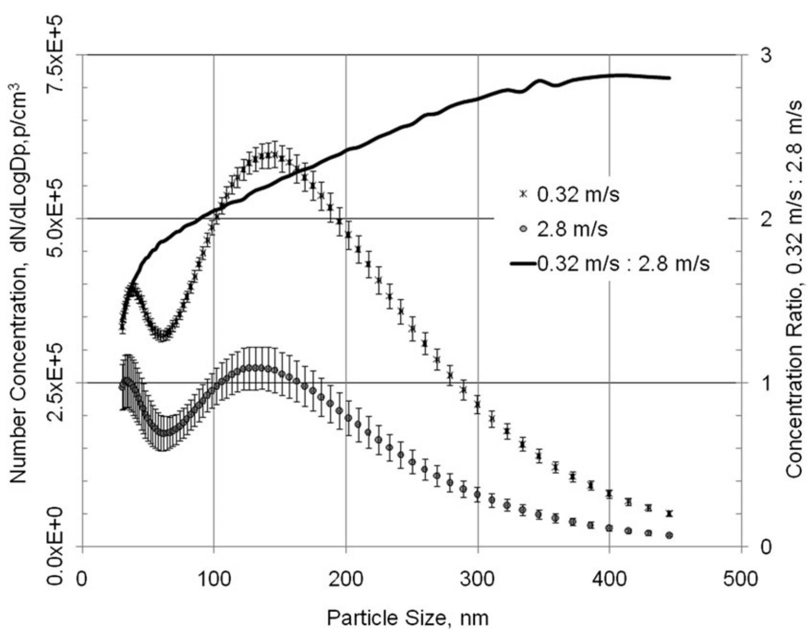

Fig. 2. Average PSDs at representative low wind velocity of 0.32 m s^{-1} and high wind velocity of 2.8 m s^{-1}, together with the ratio of concentration at 0.32 m s^{-1} to that at 2.8 m s^{-1} for each particle size from 50 nm to 445 nm. The error bars represent 1 SEM, based on replicate samples (n = 12).

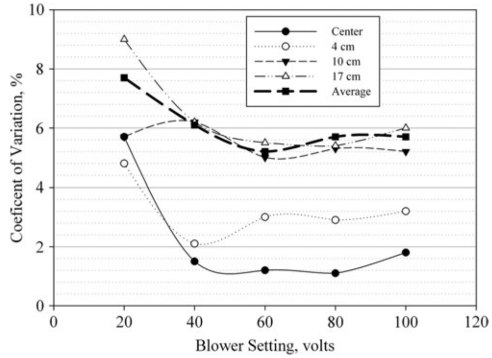

Fig. 3. CV for wind velocity at various distances from tunnel center.

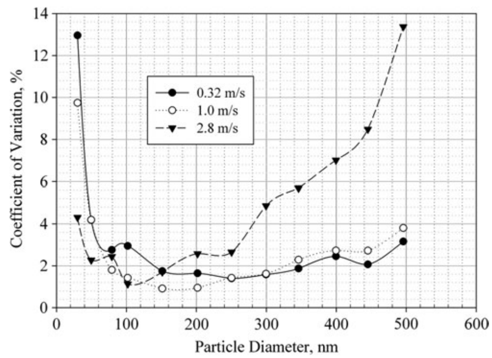

Fig. 4. CV of particle concentration as a function of particle diameter throughout cross-sectional area.

et al., 1990; Cheng et al., 2004)] and have single-pass instead of close-looped ducts (Eddins et al., 1996; Cheng et al., 2004).

Uniformity of velocity

As aforementioned, the measured velocities are within the EPA's required 10% CV. For the blower power settings of 40–100 V, CV ranges from 1.5 to 6.2%, however, CV is a bit higher for 20 V, being ~5% near the center and 9% toward the tunnel wall (see Fig. 3). For power settings between 40 and 100 V, wind velocity is most uniform at and near the center axis of the tunnel (e.g. <3% CV within 4 cm of the center and <2% at the center, while increasing to 6% near the wall), which is expected because of increases in eddy currents and turbulence caused by the wall surface. In general, for a given system, lower air velocities have lower turbulence (i.e. are more laminar), which should provide a more parabolic (i.e. less uniform) flow. Thus, as expected (Douglas et al., 2006), the results show that the 20 V power setting has slightly greater spatial variability in velocity compared to the higher power settings.

Table 1. Average wind speed (m s^{-1}) along individual sectors of the RAWT. Bold values are significantly different from center origin at $P < 0.05$

Angle	20 V	40 V	60 V	80 V	100 V
Center	0.43	1.05	1.65	2.46	3.21
22.5°	0.42	1.03	1.67	2.39	3.12
45°	0.43	1.03	1.65	2.41	3.14
90°	0.42	0.96	1.57	2.32	2.97
135°	0.38	0.94	1.54	2.25	2.92
157.5°	0.39	0.94	1.53	2.22	2.91
202.5°	0.41	**0.96**	**1.56**	**2.28**	**3.01**
225°	0.41	**0.98**	**1.58**	2.33	**3.03**
270°	0.42	1.02	1.66	2.41	3.17
315°	0.44	1.04	**1.71**	2.48	3.29
337.5°	0.44	1.06	1.71	2.50	3.29

Pooling the results into different trans-sections, quartiles, and semi-circles of different dimensions elucidates different spatial velocity profiles. Whereas the CV presented above compares individual point measures to the average, Table 1 presents the average wind speed along individual sectors of the RAWT, which is given as the angle between the indicated radial line and the vertical line (defined as 0°). Ten sectors at five power settings were tested. Using a one-tailed *T*-Test, only between one to three sectors for each setting are significantly lower ($P < 0.05$) than the wind speed at the center axis for four of five power settings, favoring a slightly lower wind speed in the rear-bottom quartile. The results at 20 V show the highest uniformity with no sectors different from the center. In total, only 8 of the 50 tested sectors, at five power settings, are significantly lower than the center wind velocity. Although the average velocity along the sectors clearly show a slight decrease within one region, other analyses by concentric regions, below, show decreases along the front wall of the RAWT.

Hence, although the results show uniformity for velocity and compare well with the U.S. EPA (1997) criteria, small departures, mostly <10% CV, are revealed. For example, Fig. 5a mostly reflects uniformity of flow, with the average wind velocity between the front and rear slightly decreasing away from the center, particularly near the wall at the highest power settings of 80 and 100 V. This effect is expected, based on generally understood fluid mechanics, and is consistent with previous studies (Ranade et al., 1990; Eddins et al., 1996). However, a more detailed evaluation along the horizontal axis (i.e. between the 90 and 270° sectors)

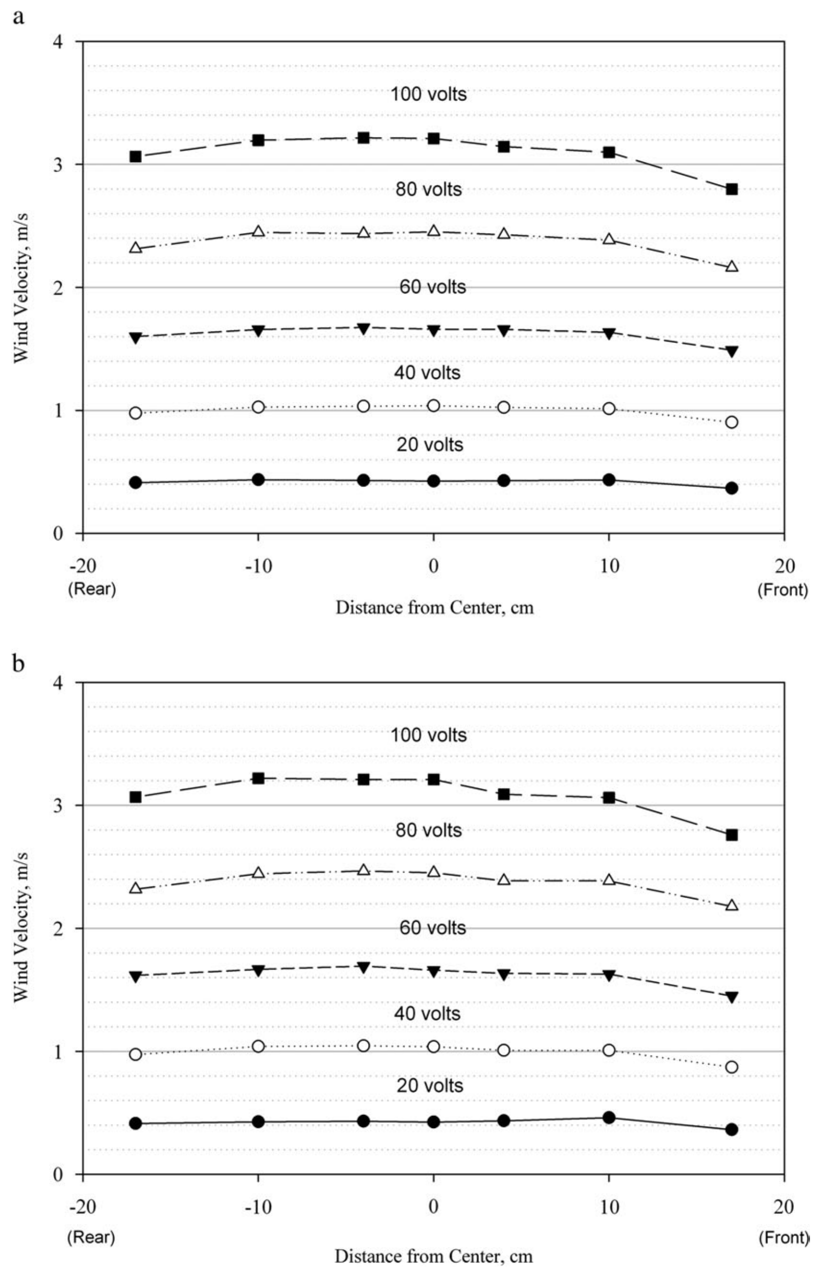

Fig. 5. Velocity for a range of blower settings at 4, 10, and 17 cm from center: (a) averaged along concentric circles of rear and front hemisphere and (b) at individual points along radial segment between the front and rear hemispheres (i.e. between 90 and 270°; see Fig. 1d).

shows slightly localized perturbations in wind speed that do not have a maximum at the center for most of the cases, except for 100 V (see Fig. 5b). This is similar to previous studies that do not show a symmetric and parabolic velocity profile across a given axis that transects the center (Ranade *et al.*, 1990; Witschger *et al.*, 1997).

To further evaluate the uniformity, wind speed is plotted along radial segments of the experimental test section at 20 and 80 V, for all three concentric regions measured (i.e. 4, 10, and 17 cm from the center axis) (see Fig. 6). Although a relatively low variability of velocity is visually observed, a slight decrease in velocity occurs toward the wall (i.e. at 17 cm from the center),

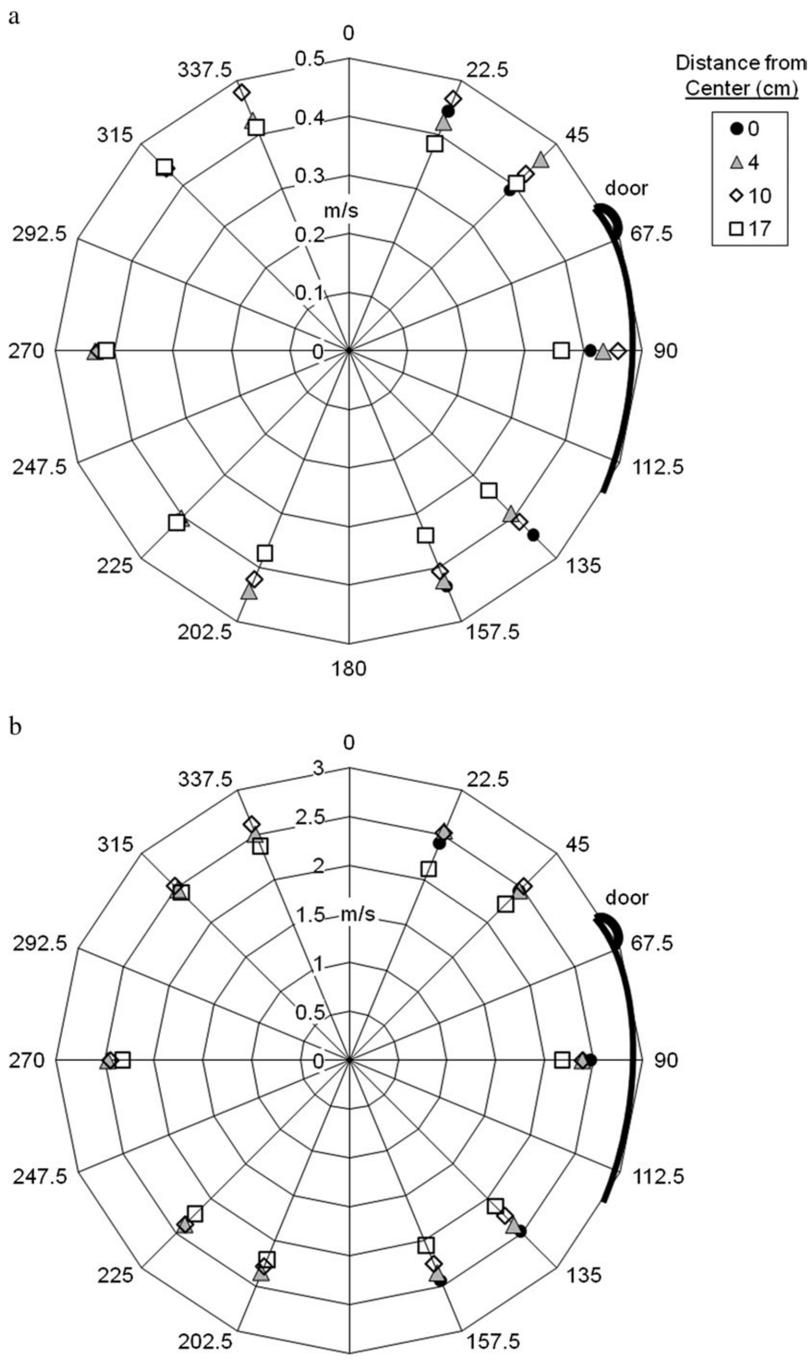

Fig. 6. Average wind velocity for points on several radial segments along three concentric circles (4, 10, and 17 cm) and at the center for blower power settings of (a) 20 V and (b) 80 V.

especially toward the front wall (22.5–157.5°). The lower values near the wall are likely due to friction that develops a boundary layer (Hinds and Kuo, 1995; Ayotte and Hughes, 2004). The radial array of velocity also reveals greater variability in velocities measured near the door than at the rear wall, which indicates subtle nonmeasureable leaks in the seal of the test section door and/or surface disruptions about the seams of the door jam. Table 1 also shows velocities near the bottom rear of the tunnel to be significantly lower ($P < 0.05$) than at the center axis and higher, albeit not significant ($P = 0.265$–0.491), at the top and right regions (22.5 and 45°). It should be noted that, since this RAWT is a first generation test unit, the door will need to be redesigned in future generations to reduce potential leaks and turbulence associated with the non-smooth surface at its seams and hinges.

Uniformity of particle concentration

As with the wind velocity profile, for particles with $_{em}D_{50}$ between 50 and 445 nm at all power settings, the overall uniformity of particle concentration is within the EPA testing criteria (i.e. CV < 10%) as shown in Fig. 4. At the lower power settings of 20 and 40 V, there is a substantially greater uniformity, showing CV to be <4.2%. Most of the increase in variability for the largest (>450 nm) and smallest (<30 nm) particle sizes, especially at the higher

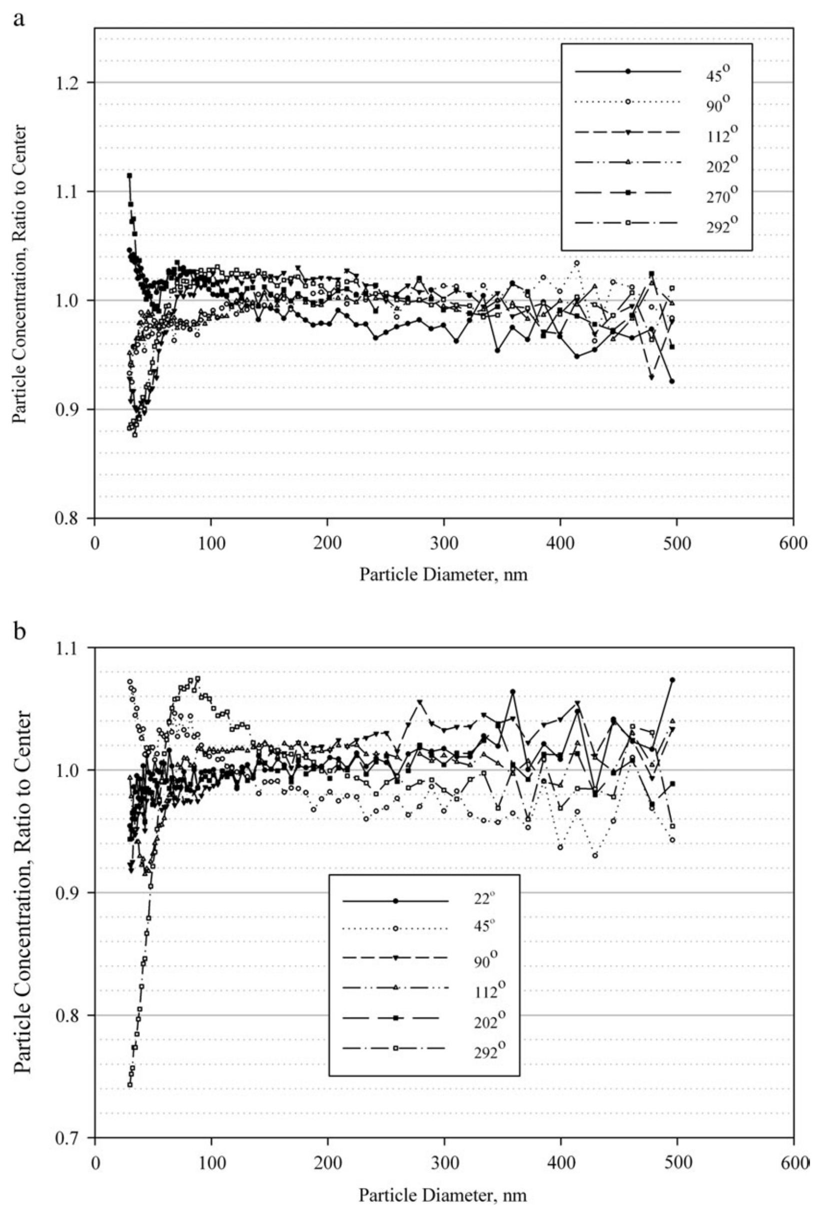

Fig. 7. Average particle concentration along segmental lines relative to center concentration for 40 V blower setting at: (a) 4 cm and (b) 7 cm from center.

power setting of 80 V, is due to much lower particle concentrations, where the relative error increases more for particles outside than it does for the particles between this range (see Fig. 2). On average, the particle concentration for 20 V continuously increases from two to three times the 80 V power setting, as particle size increases from 100 to 450 nm. Figures 7 and 8 demonstrate the spatial uniformity of particle concentration by size at 4 and 7 cm from the center axis for the 40 V power setting at all tested coordinates along individual radial segments. Overall, for particles >50 nm, low variability of <5% is observed on all locations across the tunnel.

Stability of aerosol size and concentration

The design of the RAWT was intended to maintain the aerosol concentration during the test period of 1–2 h. For 40 V, the middle wind speed tested (1.0 m s^{-1}), the evolution of aerosol concentration in the RAWT traced over time rapidly increases to ~1 000 000 p cm^{-3} during the first 5–20 min after the onset of aerosol injection (see Fig. 9). The stable

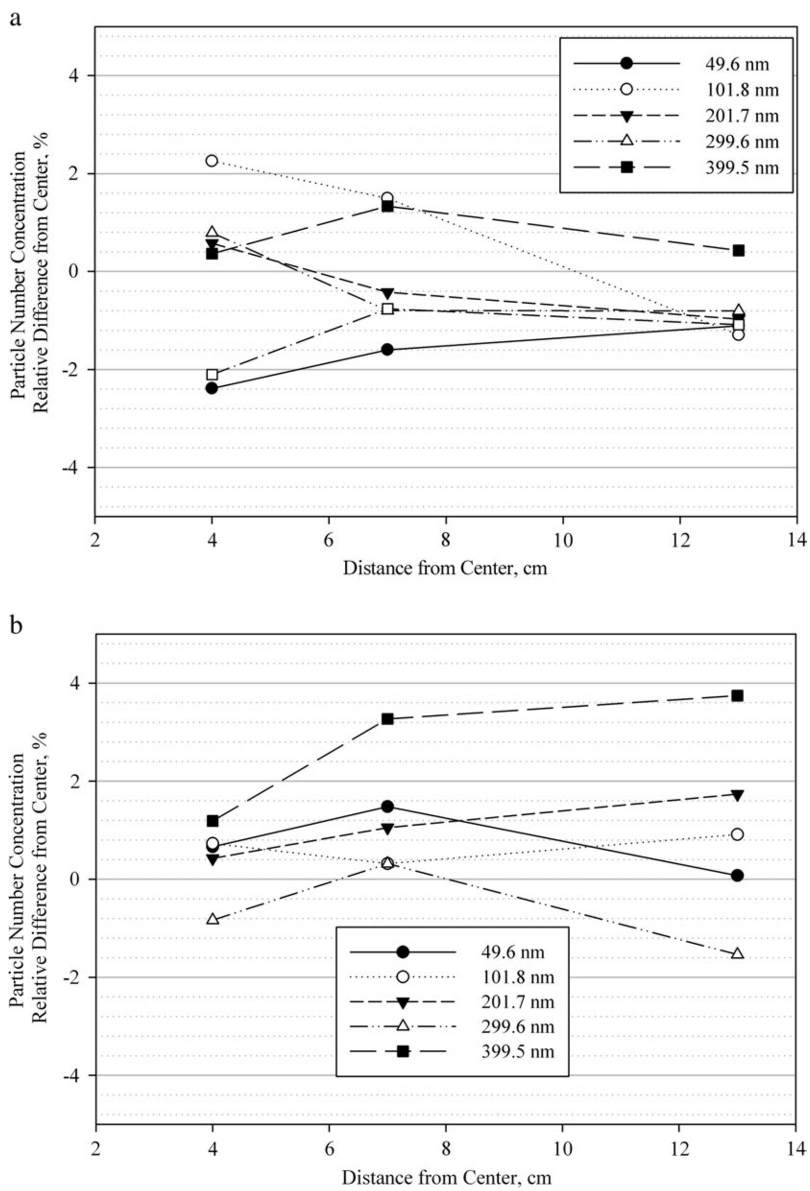

Fig. 8. Particle number concentration, relative to the concentration at the center axis at 4, 7, and 13 cm from center for (a) 20 V and (b) 80 V.

aerosol concentrations were quickly reached before commencement of a representative 66-min test, and the CMD (135 nm) and GSD (2.20) did not change significantly. For the particle concentrations studied (e.g. ranging from 1×10^5 to 10^6 p cm^{-3}), a time period between 3.5 and 34 h is required to reduce the concentration of a monodisperse aerosol to one-tenth of its original value due to agglomeration (Friedlander, 2000). In contrast, a polydisperse aerosol coagulates at a much higher rate (Hinds, 1999). Since the results show no observable coagulation at the higher concentration polydisperse aerosol, lower concentrated monodisperse aerosols intended for testing the MPAS would have much lower and likely negligible coagulation losses. Additionally, it is clear that neither were the particles enlarged nor were the concentrations lowered, as would be expected if coagulation was a significant factor. These results suggest that there was a relatively consistent aerosol, with a small enhancement of the concentration due to recirculation, that is maintained throughout the test, and, likely, coagulation was not a factor for the aerosol concentrations and time period evaluated. Furthermore, the continuous replenishment of particles would have masked and trivial agglomeration of aged aerosol.

To assess the rate of particle loss on aerosol stability, the RAWT was evaluated for a 2-h period at two velocities (0.5 and 1.2 m s^{-1}) without injection

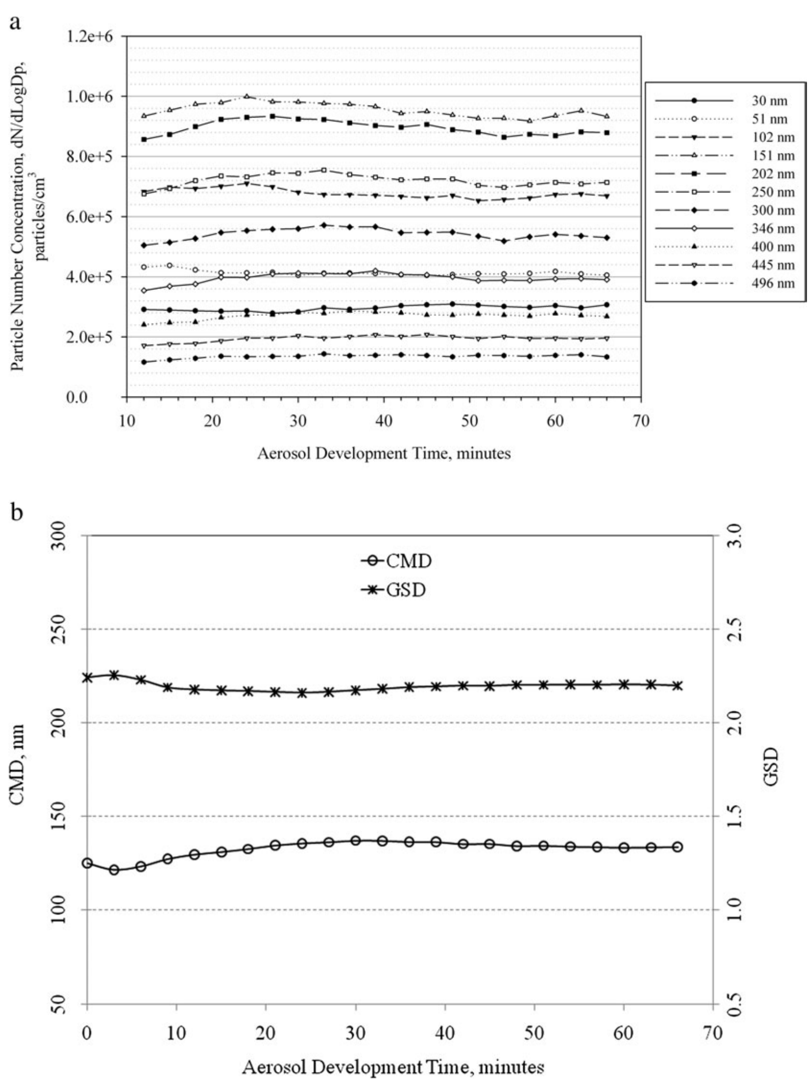

Fig. 9. Evolution of polydisperse aerosol in RAWT during injection of fresh aerosol and recirculation by: (a) single particle size and (b) count median diameter (CMD) and geometric standard deviation (GSD).

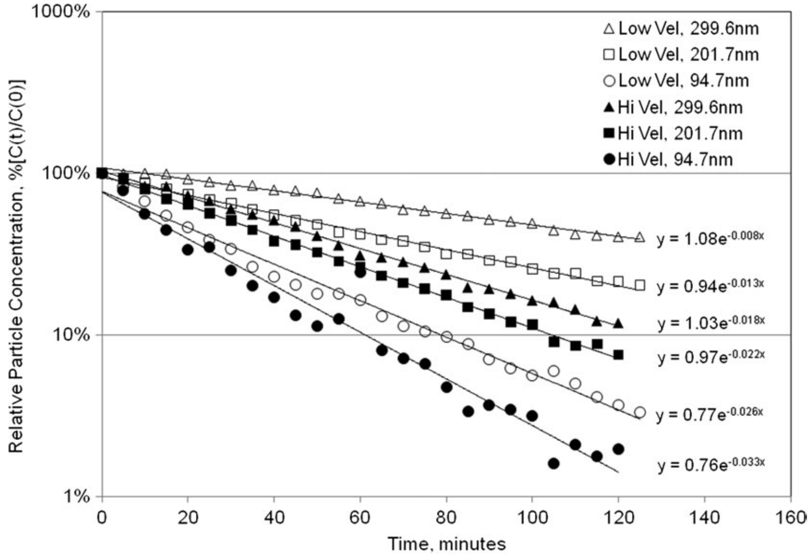

Fig. 10. Particle deposition rates velocities of 0.5 and 1.2 m s^{-1} without replenishment, conducted after steady state aerosol concentration was established.

of fresh aerosol. This evaluation was conducted after steady state aerosol concentrations were established. The deposition pattern followed a logarithmic decay rate. The slope was derived from the exponent of the regression equation, which defines the rate of deposition. The results show that the deposition rate increases with decreases in particle size (see Fig. 10). This trend can be explained by Brownian diffusion (Chen and Ahmadi, 1997). By increasing velocity from 0.5 to 1.2 m s^{-1}, the deposition rate increases by factors of 1.3, 1.7, and 2.3 for 95, 202, and 300 nm particles, respectively. This can partially be explained by an increase in particle deposition caused by an increase in turbulent diffusion at higher velocities (Hadj and Ahmadi, 1990). The exponential decay rate observed in this study follows the curve shape for particle settling with mixing in a chamber without aerosol replenishment (Hinds, 1999). However, in this study, particle losses were likely by diffusion not gravitational settling; the models are similar because the settling velocity in the stirred settling model can be replaced with an equivalent diffusion velocity.

SUMMARY AND CONCLUSIONS

Generally, the results show that the airflow and PSD are uniform and compare well with other studies, including the U.S. EPA's criteria for testing PM10 monitors. A high level of uniformity was found with a CV of 1.5–6.2% for wind velocities between 0.4 and 2.8 m s^{-1} and, in this range, for particles with ${}_{em}D_{50}$ between 50 and 450 nm, a CV of 0.8–8.5%. For a given blower power, a time series evaluation of the PSD suggests that both growth of particle size from agglomeration and losses because of diffusion were negligible, while the recirculation and replenishment design maintained the overall particle concentration. It is concluded that this recirculation wind tunnel maintains a uniform airflow and uniform and stable aerosol, all useful for measuring particle penetration through protective clothing materials and conducting tests on passive aerosol samplers at various wind speeds and directions.

Acknowledgements—The authors are thankful to Drs Aleksandar Bugarski, Chaolong Qi, and Benjamin Eimer at National Institute for Occupational Safety and Health (NIOSH) for their review of the manuscript and suggestions. We thank Ms Christiana Lee, a summer student from University of Florida College of Engineering for her help in preparation of this manuscript.

Disclaimer—The findings and conclusions of this report are those of the author(s) and do not necessarily represent the views of the NIOSH.

REFERENCES

Aizenberg V, Choe K, Grinshpun SA *et al*. (2001) Evaluation of personal aerosol samplers challenged with large particles. J Aerosol Sci.; 32: 779–93.

ANSI. (1999) Sampling and monitoring for releases of airborne radioactive substances from the stacks and ducts of nuclear facilities. ANSI N13.1. New York, NY: American National Standards Institute.

Ayotte KW, Hughes DE. (2004) Observations of boundary-layer wind-tunnel flow over isolated ridges of varying steepness and roughness. Boundary-Layer Meteorol; 112: 525–56.

Bergman W, Garr J, Fearon D. (1989) Aerosol penetration measurements through protective clothing in small scale simulation tests. Lawrence Livermore National Laboratory. Presented at: 3rd International Symposium on Protection against Chemical Warefare Agents, Umeå, Sweden, June 11–16.

Chen Q, Ahmadi G. (1997) Deposition of particles in turbulent pipe flow. Aerosol Sci Technol; 28: 789–96.

Cheng Y, Irshad H, McFarland A *et al*. (2004) An aerosol wind tunnel for evaluation of massive-flow air samplers and calibration of snow white sampler. Aerosol Sci Technol; 38: 1099–107.

Dandy DS, Yun J. (1997) Momentum and thermal boundary-layer thickness in a stagnation flow chemical vapor deposition reactor. J Mater Res; 12: 1112–21.

Douglas JF, Gasiorek JM, Swaffield JA *et al*. (2006) Fluid mechanics. 5th edn. Englewood Cliffs, NJ: Prentice Hall; ISBN-10: 0131292935.

Eddins PM, Gao P, Dillon HK *et al*. (1996) A compact wind tunnel for evaluating aerosol samplers, Appl Occup Envrion Hyg; 11: 44–55.

Friedlander SK. (2000) Smoke, dust, and haze, fundamentals of aerosol dynamics. 2nd edn. New York, NY: Oxford University Press, Inc.

Gao P, Jaques PA, Hsiao T-C *et al*. (2011) Evaluation of nano- and sub-micron particle penetration through ten nonwoven fabrics using a wind-driven approach. J Occup Environ Hyg; 8: 13–22.

Hadj O, Ahmadi G. (1990) A comparison of brownian and turbulent diffusion. Aerosol Sci Technol; 13: 47–53.

Hinds WC, Kuo T-L. (1995) A low velocity wind tunnel to evaluate inhalability and sampler performance for large dust particles. Appl Occup Environ Hyg; 10: 549–56.

Hinds WC. (1999) Aerosol technology: properties, behavior, and measurement of airborne particles. 2nd edn. New York, NY: Jon Wiley & Sons, Inc.

Institute of Environmental Sciences and Technology (IEST). (2003) IEST-RP-CC003.3: Garment system considerations for cleanrooms and other controlled environments. Arlington Heights, IL: Institute of Environmental Sciences and Technology.

Liden G, Kenny LC. (1994) Errors in inhalable dust sampling for particles exceeding 100 μm. Ann Occup Hyg; 38: 373–84.

Peters TM, Leith D. (2004a) Modeling large-particle deposition in bends of exhaust ventilation systems. Aerosol Sci Technol; 38: 1171–77.

Peters TM, Leith D. (2004b) Measurement of particle deposition in industrial ducts. J Aerosol Sci; 35: 529–40.

Peters TM, Leith D. (2004c) Particle deposition in industrial duct bends. Ann Occup Hyg; 48: 483–90.

Ranade MB, Woods MC, Chen F-L *et al*. (1990) Wind tunnel evaluation of PM10 samplers. Aerosol Sci Technol; 13: 54–71.

U.S. Army Dugway Proving Ground UT. (1997) Test operations procedure (TOP) 8-2-501, permeation and penetration of air-permeable, semipermeable, and impermeable materials with chemical agents or simulants. Advanced Materials, Manufacturing, and Testing Information Analysis Center (AMMTIAC), Dugway, UT.

U.S. EPA. (1987) Ambient air monitoring reference and equivalent methods, test procedure: subpart D—procedures for testing performance characteristics of methods for PM10. 40 CFR, 53.43, Code of Federal Regulations. Washington, DC: U.S. Government Printing Office.

U.S. EPA. (1997) Ambient air monitoring reference and equivalent methods, test procedure: subpart F—full wind tunnel test. 40 CFR, 53.62, Code of Federal Regulations. Washington, DC: U.S. Government Printing Office.

Wagner J, Leith D. (2001) Passive aerosol sampler. Part I: principle of operation. Aerosol Sci Technol; 34: 186–92.

Witschger O, Wrobel R, Fabries JF *et al*. (1997) A new experimental wind tunnel facility for aerosol sampling investigations. J Aerosol Sci; 28: 833–51.